JOURNAL OF AGRICULTURAL AND FOOD CHEMISTRY

Photodegradation of Fenitrothion and Parathion in Tomato Epicuticular Waxes

MASAO FUKUSHIMA* AND TOSHIYUKI KATAGI

Environmental Health Science Laboratory, Sumitomo Chemical Co., Ltd., 2-1, Takatsukasa 4-chome, Takarazuka, Hyogo 665-8555, Japan

Photodegradation of ^{14}C-labeled fenitrothion ([*O*,*O*-dimethyl *O*-(3-methyl-4-nitrophenyl) phosphorothioate]) and parathion ([*O*,*O*-diethyl *O*-(4-nitrophenyl) phosphorothioate]) was conducted on a series of solid surfaces including isolated tomato fruit and leaf cuticle waxes. The wax-coated glass plate gave the comparative degradation of fenitrothion observed for the intact plant but both surfaces of octadecyl-capped silica gel and poly(tetrafluoroethylene) enhanced its volatilization. Photoinduced desulfuration and ester cleavage were common to both pesticides in waxes, but formation of the azo derivative was found to be a major degradation pathway characteristic of parathion. The modified electronic states of the nitro group by introduction of *m*-methyl group accounted for this different photoreactivity based on molecular orbital calculations.

KEYWORDS: Fenitrothion; parathion; photodegradation; epicuticular wax

INTRODUCTION

The fate of a pesticide especially when sprayed on crops is complex, but the primary event should be incorporation into plant epicuticular wax (*1*) followed by penetration to plant tissues through the wax and cutin layers. The photochemical reactions are known to be one of the most important factors determining the fate of pesticides on a plant surface as well as volatilization (*2*). In plant tissues, pesticide molecules undergo various types of primary transformation in the aid of enzymes, and the metabolites are further conjugated with natural products. By the way, the potential degradates and metabolites of a pesticide as well as their residues are examined in plant metabolism study, and analytical targets in the crop residue trials for registration are determined. In general, the transformation of pesticide in plant is obtained as a total degradation on the plant surface and metabolism in plant tissues. To examine the surface phenomena separated from the metabolism in tissues, surface wash by organic solvents is usually undertaken in metabolism studies, but incomplete recovery of penetrated species can be supposed. As an alternative approach, some plant surface models using methyl oleate (*3*), cyclohexene (*4*), cellulose and silica gel (*5*) and poly(tetrafluoroethylene) plate (*6*) have been examined by many researchers in relation to photodegradation. The extracted plant epicuticular waxes (*7*−*9*) and enzymatically isolated plant cuticles (*10*) were also utilized to investigate the photolysis of pesticides on a plant surface.

By the way, fenitrothion [**I**; *O*,*O*-dimethyl *O*-(3-methyl-4-nitrophenyl) phosphorothioate] has been reported to undergo photoinduced thiono−thiolo rearrangement, oxidative desulfuration, and cleavage of the P−O aryl linkage (*11*−*13*). In contrast, parathion [**IV**; *O*,*O*-diethyl *O*-(4-nitrophenyl) phosphorothioate], having a chemical structure very similar to that of **I**, has been reported to undergo photoreduction of the nitro group, leading to formation of azo and azoxy derivatives besides the oxidation in the presence of cyclohexene, methyl oleate, or 12-hydroxystearate or on isolated paprika cuticles (*3*, *4*, *14*). Similar photoreduction with subsequent reactions has never been reported for **I**, and hence, it is not clear whether this difference originates from the different photoreactivities between **I** and **IV** or simply being missed in the detection by usual analytical methods.

Based on these considerations, the comparative photolysis study of **I** and **IV** was conducted on glass surface in the presence and absence of epicuticular waxes from tomato fruits and leaves to investigate the product profiles. The difference in photochemical reactivity between **I** and **IV** was also theoretically examined by using molecular orbital (MO) calculations. Furthermore, several systems such as silica gel, octadecyl-modified silica gel, and poly(tetrafluoroethylene) film were examined as plant surface models through photodegradation of **I**.

MATERIALS AND METHODS

Chemicals. Fenitrothion, its oxon derivative [**II**; *O*,*O*-dimethyl *O*-(3-methyl-4-nitrophenyl) phosphate], and *S*-methyl isomer [**III**; *O*-methyl *S*-methyl *O*-(3-methyl-4-nitrophenyl) phosphorothiolate], and parathion and its oxon derivative [**V**; *O*,*O*-diethyl *O*-(4-nitrophenyl) phosphate] were synthesized in our laboratory according to the reported methods (*11*, *12*). The azo derivatives of **I** [**VI**; 4,4′-bis(dimethoxyphosphinothioyloxy)-2,2′-dimethylazobenzene] and of **IV** [**VII**; 4,4′-bis(diethoxyphosphinothioyloxy)azobenzene] were also synthesized from 3-methyl-4-nitrophenol (**VIII**) and 4-nitrophenol (**IX**), respectively, by the reported method using Zn and NaOH (*14*). Crude **VII** was purified by silica gel column chromatography using methanol/chloroform, and purity was 98.3%. Amino derivatives of **I** [**X**; *O*,*O*-dimethyl *O*-(3-

10.1021/jf052113d CCC: $33.50
Published on Web 12/27/2005

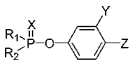

Compd.	R_1	R_2	X	Y	Z
I	OCH_3	OCH_3	S	CH_3	NO_2
II	OCH_3	OCH_3	O	CH_3	NO_2
III	OCH_3	SCH_3	O	CH_3	NO_2
IV	OCH_2CH_3	OCH_2CH_3	S	H	NO_2
V	OCH_2CH_3	OCH_2CH_3	O	H	NO_2
X	OCH_3	OCH_3	S	CH_3	NH_2
XI	OCH_2CH_3	OCH_2CH_3	S	H	NH_2

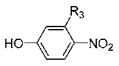

Compd.	R_3
VIII	CH_3
IX	H

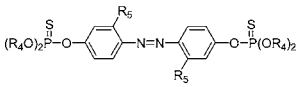

Compd.	R_4	R_5
VI	CH_3	CH_3
VII	CH_2CH_3	H

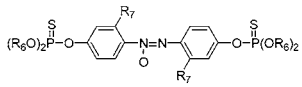

Compd.	R_6	R_7
XII	CH_3	CH_3
XIII	CH_2CH_3	H

Figure 1. Chemical structures of test compounds (**I** and **IV**) and authentic standards.

methyl-4-aminophenyl) phosphorothioate] and **IV** [**XI**; *O*,*O*-diethyl *O*-(4-aminophenyl) phosphorothioate] were prepared by reduction of **I** and **IV**, respectively (*15*, *16*). The azoxy derivative of **I** [**XII**; 4,4′-bis((dimethoxyphosphinothioyl)oxy)-2,2′-dimethylazoxybenzene] and **IV** [**XIII**; 4,4′-bis((diethoxyphosphinothioyl)oxy)azoxybenzene] were synthesized directly from **I** and **IV** by treatment with zinc powder and acetic anhydride in acetic acid (*14*). The chemical structure of all of them is shown in **Figure 1**. [^{14}C]**I** (6.66 MBq mg^{-1}) and **IV** (1.27 MBq mg^{-1}) uniformly labeled with ^{14}C in the phenyl ring were prepared in our laboratory (*17*) and purchased from Muromachi Yakuhin Kaisha Ltd. (Tokyo, Japan), respectively. Their radiochemical purity was determined to be greater than 98% by HPLC.

Silica gel (60, 70−230 mesh, E. Merck), silica gel whose silanol groups are capped with octadecyl moiety (ODS; Wakosil 40C18, Wako Pure Chemicals, Japan), poly(tetrafluoroethylene) sheet (1 mm thickness, Takiron Co. Ltd., Japan), and cyclohexane were used without any purification.

Spectroscopy. NMR spectra were measured in $CDCl_3$ by a Varian Unity-300 FT-NMR spectrometer operating at 299.94 MHz for proton NMR measurement equipped with a 4-Nucleus auto NMR probe, using tetramethylsilane as an internal standard. Liquid chromatography-electrospray ionization-mass spectrometry (LC-ESI-MS) in positive and negative ion mode was performed by Thermo Finnigan TSQ quantum spectrometer being connected to an Agilent 1100 series HPLC, and also by a Waters ZQ 2000 spectrometer with ESCi multimode probe being connected to a Waters Aliance HPLC system. Samples dissolved in a mixture of methanol and water were injected into an ion source using an autosampler at ambient temperature with a flow rate of 0.2 mL min^{-1} using a solvent mixture of methanol and water (50/50, v/v) as a mobile phase. IR spectra of **I**, **IV**, and epicuticular waxes of tomato fruit and leaf were measured by a Perkin-Elmer SpectrumOne FT-IR spectrometer equipped with a Universal ATR sampling accessory. The molecular interactions between **I** (or **IV**) and wax components were also examined by IR difference spectra by using the desiccated mixture prepared from chloroform solution of pesticide and wax (1:10, w/w). UV−vis spectra of **I** and **IV** in cyclohexane at 0.1 mmol L^{-1} were obtained using a Shimadzu UV-2550 UV−visible spectrometer in a quartz cuvette (1 cm path length). The UV−vis spectra of the isolated epicuticular waxes were also measured at the concentration of 0.30 mg mL^{-1} in *n*-hexane.

The spectroscopic data of **VI** were as follows. MS (*m*/*z*): 491 ([M + H]$^+$), 367 ([M − P(=S)$(OCH_3)_2$ + H]$^+$). NMR ($CDCl_3$): δ 7.63 (2H, d, J = 8.7, Ph-H), 7.14 (2H, brd, Ph-H), 7.07 (2H, brd, J = 9.0, Ph−H), 3.89 (12H, d, J = 13.5, -OCH_3), 2.72 (6H, s, Ar−CH_3). IR (ATR, cm^{-1}): 3375, 2952, 2921, 1599, 1583, 1484, 1225, 1033, 967, 831. The MS spectrum of **XII** was as follows. MS (*m*/*z*): 529 ([M + Na]$^+$), 507 ([M + H]$^+$), 246 ([$(CH_3O)_2$P(=S)$OC_6H_3(CH_3)$N + H]$^+$).

Radioassay. Radioactivity in rinsate from the various surfaces used as carrier of pesticide was determined by mixing each aliquot with 10 mL of Packard Emulsifier Scintillator Plus and analyzed by liquid scintillation counting (LSC) with a Packard Model 1600TR, 2000CA, and 2900TR being equipped with an automatic external standard. The background level of radioactivity in LSC was 30 dpm which was subtracted from the disintegrations per minute value of a measured sample. The remaining radioactivity after the extraction of wax components and silica gel was subjected to combustion analysis with a Packard oxidizer 307. The radioactivity which was trapped in a polyurethane (PU) foam plug was soaked by methanol, and its 1-mL aliquot was subjected to radioanalysis by LSC. Each aliquot (2−5 mL) from alkaline and ethylene glycol traps was also analyzed by LSC.

Chromatography. High-performance liquid chromatography (HPLC) was conducted using a Hitachi L-6200 pump linked in series with an L-4000 UV detector, D-7000 Advanced HPLC system manager, and Packard Flow-one/Beta A-120 radiodetector equipped with a 500 μL liquid cell, where Ultima-Flo AP (Perkin-Elmer) was utilized as a scintilator. A Sumipax ODS A-212 column (150 mm × 6 mm i.d., 5 μm, Sumika Chemical Analytical Service Co., Ltd.) was employed for an analytical purpose at a flow rate of 1 mL min^{-1}. The following solvent program was used for representative analysis of the degradates: 0 min, %A (0.01% trifluoroacetic acid):%B (acetonitrile):%C (methanol), 80:15:5; 0−30 min, linear, 10:70:20 at 30 min; 30−45 min, linear, 5:75:20 at 45 min; 45−50 min, linear, 0:80:20 at 50 min; 50−60 min, isocratic. Chemical identification of each degradate was conducted by HPLC cochromatography with authentic standards.

Thin-layer cochromatography (TLC) with authentic standards was conducted using silica gel 60F_{254} thin-layer chromatoplates (20 cm × 20 cm, 0.25 mm thickness, Merck) using the solvent system of toluene:ethyl acetate:acetic acid = 5:7:1 (v/v/v) for development. The non-radiolabeled reference standards were detected by exposing TLC plates to ultraviolet light or iodine vapor. Autoradiograms were prepared by exposing TLC plates to BAS-IIIs Fuji Imaging Plates for several hours. The radioactivity on an imaging plate was analyzed by a Fuji Bio-Imaging Analyzer BAS-1500. The typical HPLC retention times by method 2 and TLC R_f values are listed in **Table 1**.

Table 1. Retention Times (HPLC) and R_f Values (TLC) of Test Substances and Reference Compounds

compd	HPLC t_R (min)	TLC R_f Value
I	29.9	0.69
II	20.9	0.44
III	23.2	0.50
IV	32.3	0.72
V	23.6	0.48
VI	39.1	0.72
VII	41.7	0.75
VIII	19.3	0.53
IX	16.7	0.54
X	17.3	0.53
XI	19.9	0.51
XII	36.0	0.70
XIII	32.3	0.71

Epicuticular Waxes. Tomato seedlings in the fourth leaf stage (*Lycopersicon esculentum* Mill., cv. Ponterosa) were grown in compost (Kureha Chemical Co., Ltd., Tokyo) in 0.02 m^2 Wagner pots with magnesia lime. Tomato plants were maintained in a greenhouse (August−October, 2001) at 25/20 °C for day/night and appropriately watered until harvest. The leaves were cut from petiole at BBCH 65−70 (full flowering − first fruit visible) and amounted to 493 g (563 leaves), and 2.3 kg (29 fruits) were harvested at BBCH 80−89 (begging of ripening − fully ripe) (*18*). The collected leaves and fruits were individually immersed in chloroform for approximately 2 min (*19*). Then, the chloroform solution was concentrated under the reduced pressure, and these collected epicuticular waxes from leaf and fruit were used without purification for the photolysis study.

Photolysis Study. The thin film of epicuticular waxes was prepared in the bottom of the inner surface of a small Pyrex Petri dish (2.8 cm i.d. × 1.5 cm height) as its density became close to that estimated for tomato plant grown in the greenhouse: 0.032 mg cm^{-2} (fruit); 0.074 mg cm^{-2} (leaf). The 1 mL aliquot of chloroform solution of each epicuticular wax was added to a Petri dish, and the organic solvent was allowed to evaporate in the dark overnight. [^{14}C]**I** or **IV** in acetonitrile solution (100 μL, ca. 0.03 MBq) was evenly applied to a Petri dish as a small (~1.0 mm diameter) droplet with or without the wax film using a Hamilton microsyringe at a rate of 7.5 μg cm^{-2} according to good agricultural practice. The dishes were kept in the dark for 2 h until the solvent evaporated. These Petri dishes placed into the cylindrical photoreaction vessel covered with a Pyrex glass were irradiated with a 2 kW xenon arc lamp (Ushio, Tokyo) whose spectral irradiance was very similar to natural sunlight according to the reported method (*20*). CO_2-free air being saturated with water vapor passed over the irradiated samples at a flow rate of about 0.1 L min^{-1} to the polyurethane foam plug covered with aluminum foil; a gas-washing bottle containing 100 mL of ethylene glycol and the another one containing 100 mL of 1 M NaOH were lined in series to trap volatile ^{14}C. The temperature at the sample surface was maintained at 25 ± 1 °C by passing thermostated water below the bottom of the photoreaction vessel. The dark control samples were examined in the same way except the light.

At appropriate intervals, the five Petri dishes were removed from the photoreaction vessel. Each Petri dish was rinsed with 20 mL of a mixture of chloroform and hexane, and the inner surface of the photoreaction vessel and Pyrex cover were also washed individually with 20 mL of methanol. The recovered ^{14}C from the polyurethane foam plug was soaked with 50 mL of methanol. The portion of each fraction was radioassayed in duplicate by LSC. A 1 mL aliquot of ethylene glycol and 1 M NaOH in the gas-washing bottles were separately radioassayed in a similar manner. The 10 mL aliquot of 1 M NaOH in the alkaline trap was treated with 10 mL of 2 M $BaCl_2$ to precipitate $Ba^{14}CO_3$, which was separated by centrifugation, and a portion of the supernatant was radioassayed in duplicate to quantify $^{14}CO_2$.

To examine the effect of epicuticular wax, the several carriers were subjected to photodegradation of **I** in addition to the glass surface. Silica gel has been previously used as a convenient carrier, but its reactive silanol group on the surface may affect the photoreactivity of **I**. Since epicuticular wax is known to contain alkanes and alcohols having long alkyl chains (*21*), silica gel whose silanol groups are capped with an octadecyl moiety (ODS) was utilized as a simple model of epicuticular wax together with the usual silica gel as control. As previously reported by Peacock et al. (*6*), a poly(tetrafluoroethylene) sheet was additionally used as another model surface. By considering the maximum photic depth in soil reported by Frank et al. (*22*), the thickness of the silica gel and ODS was adjusted to 0.5 mm. The appropriate amount of each silica gel (154−162 mg) was weighed in a Petri dish by taking account of their density (0.50−0.53 mg cm^{-3}). To these surfaces, acetonitrile solution of [^{14}C]**I** was evenly applied and a photodegradation study was conducted similarly to that of the epicuticular wax surface. Furthermore, the photodegradation study of [^{14}C]**I** in cyclohexane at 1 ppm was also conducted by using the same irradiation apparatus but in 50 mL beaker, since organic solvents have been examined as the simplest surrogate of epicuticular wax (*2*). All photodegradation study was conducted in five replicates.

Molecular Orbital Calculations. The initial molecular geometries of **I** and **IV** were derived from the standard values of bond lengths and angles. There are many possible conformers originating from rotation around one P−O aryl and two P−O alkyl bonds, and hence, the gauche configuration with torsional angles of around 50° were conveniently taken according to ab initio calculations on *O*,*O*-dimethyl *O*-phenyl phosphorothioate (*23*). The molecular geometries were then fully optimized by the PM3 molecular orbital (MO) calculations, using the WINMOPAC program (version 2.0, Fujitsu Ltd.) (*24*). To examine the electronic configurations of **I** and **IV** in the excited singlet states, the PM3-optimized geometries were subjected to CNDO/S MO calculations (*25*) using the MOS-F program (version 4.1) in WINMOPAC by taking account of configuration interaction (CI) of the lowest 100 configurations (*24*). The electronic transitions most likely to be involved in photolysis of **I** and **IV** were evaluated by comparing the predicted absorption maximum and their oscillator strength with those measured in UV−vis spectroscopy.

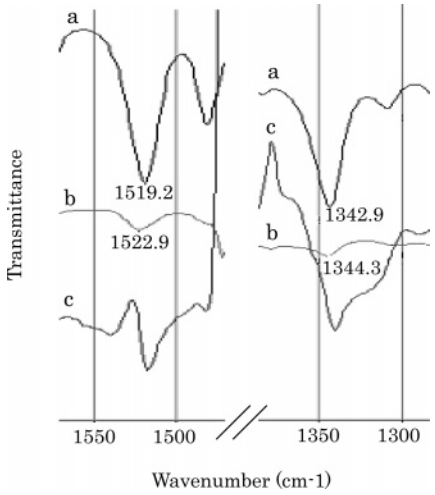

Figure 2. FT-IR spectra of fenitrothion (**I**): (**a**) fenitrothion; (**b**) fenitrothion mixed with epicuticular wax of tomato fruit; (**c**) differential spectrum of **a** and **b**.

RESULTS

Spectroscopy. The UV absorption spectra of **I** and **IV** in cyclohexane exhibited absorption at 262.5 nm (ϵ = 10 880 M^{-1} cm^{-1}) and 269 nm (ϵ = 10 770 M^{-1} cm^{-1}), respectively, possibly due to a $\pi \rightarrow \pi^*$ transition at the phenyl ring. Their shoulder extended to wavelengths of >280 nm, and significant absorption at 290 nm (ϵ = 5030 and 5690 M^{-1} cm^{-1} for **I** and **IV**) implied the possible photolysis in homogeneous media under the exposure conditions used in this study. The isolated epicuticular wax in *n*-hexane did not show any significant absorbance at >250 nm, but the extracted leaf waxes had slight absorption at 267.0 and 371.5 nm. These profiles are similar to those from citrus fruits reported by Pirisi et al. (*7*).

The FT-IR spectra of **I** and **IV** exhibited asymmetric stretching of the nitro group at 1519 and 1521 cm^{-1} and its symmetric stretching at 1343 and 1345 cm^{-1}, respectively, showing the insignificant effect by the *m*-methyl group in the phenyl ring, as shown in **Figure 2**. The IR spectrum of the epicuticular wax of tomato fruit and leaf showed a strong and broad absorption due to O−H stretching at 3285−3347 cm^{-1}, C−H stretching at 2849−2916 cm^{-1}, and C−O stretching at 1261 cm^{-1}, which implied the presence of alkane and alcohol species in the epicuticular waxes (*21*). In the case of fruit waxes, the IR absorption at 1711 cm^{-1} was observed and the presence of an ester moiety is considered. The stretching of the nitro N−O bonds was modified by coexistence of the fruit epicuticular waxes, and the corresponding asymmetric and symmetric absorption of N−O bonds were shifted to 1523 and 1344 cm^{-1} (**I**) and 1525 and 1346 cm^{-1} (**IV**), respectively (**Figure 2**). Almost similar shifts were observed when the leaf epicuticular waxes were used. These shifts to a higher wavenumber, especially for asymmetric N−O stretching of the nitro group, suggested some molecular interactions between **I** and the epicuticular waxes via this functional group.

Photolysis. The amount of **I** remaining on the Petri dish gradually decreased during 8 h exposure to artificial light, depending on the carrier used, as shown in **Figure 3**. The ^{14}C recovery throughout the study was 88.9−113.2% of the applied ^{14}C. The dissipation half-lives of **I** from the Petri dish were

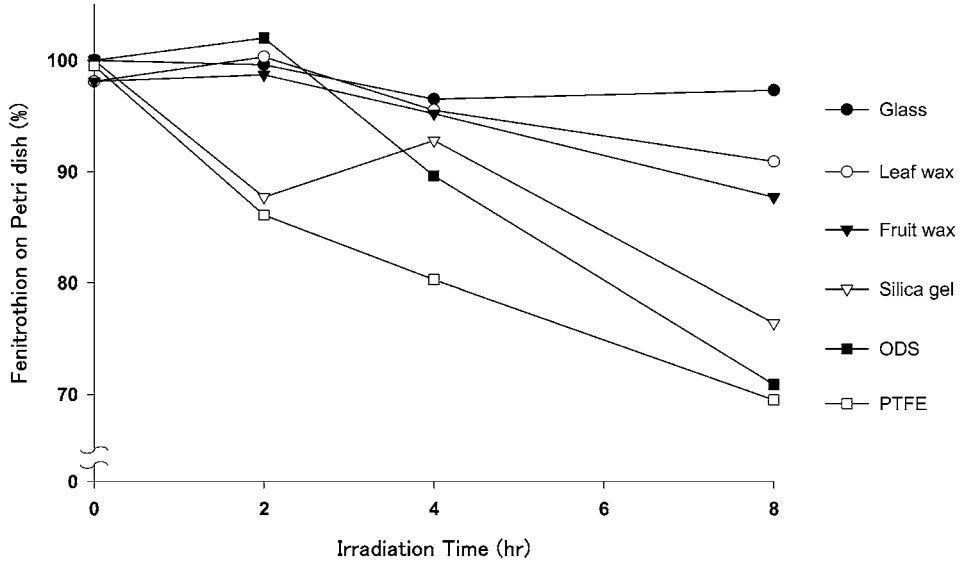

Figure 3. Rate of photodegradation of fenitrothion (**I**) in Petri dishes containing waxes.

Table 2. Photodegradation of Fenitrothion (**I**) On/In Various Media

	% of the applied ^{14}C					
compd	glass	leaf wax	fruit wax	silica gel	ODS[d]	PTFE[e]
Petri dish						
I	97.3	90.9	87.7	76.4	70.8	85.2
II		0.6	0.3	1.0	1.0	
III			0.7			
VIII		0.5	0.3			
others[a]		1.5	7.5	9.9	0.8	
vessel wall						
I	0.6	0.6	0.1	0.1	8.6	17.2
others[a]	0.3	0.3	0.2	<0.1	<0.1	0.4
PU[b]						
I	0.1	<0.1				2.2
others[a]	0.2	0.3	0.2			0.5
volatile						
EG[c]					<0.1	
NaOH	0.3	0.2	<0.1	0.8	0.9	<0.1
bound				0.7	6.6	
total ^{14}C	98.8	94.9	97.2	88.9	89.0	105.6

After 8 h exposure. [a] **VI**, **X**, and **XII** could not be detected. [b] Polyurethane foam. [c] Ethylene glycol. [d] Octadecylsilane. [e] Poly(tetrafluoroethylene).

Table 3. Photodegradation of Parathion (**IV**) on Glass and Isolated Epicuticular Wax of Tomato

	% of the applied ^{14}C		
compd	glass	leaf wax	fruit wax
Petri dish			
IV	72.0	83.7	79.3
V	2.6	1.4	1.9
VII		4.2	4.9
IX	0.5		
others[a]	5.7	4.8	2.7
vessel wall			
IV	4.8	0.9	2.0
others[a]	0.5		0.6
PU[b]			
IV	0.8	1.2	1.0
others[a]	0.3		
volatile			
EG[c]	<0.1	0.2	<0.1
NaOH	0.3	0.4	0.3
total	88.1	96.9	92.8

After 8 h exposure. [a] **XI** and **XIII** could not be detected. [b] Polyurethane. [c] Ethylene glycol.

calculated by assuming first-order kinetics to be 7.5 (glass), 2.6 (leaf wax), 1.9 (fruit wax), 0.96 (silica gel), 0.61 (ODS), 0.67 (PTFE), and 15.5 days (cyclohexane). On glass in the presence or absence of tomato epicuticular waxes and in cyclohexane, approximately more than 90% of the applied ^{14}C remained as **I** unchanged but in other cases more dissipations of **I** were observed, as listed in **Table 2**. During 8 h exposure, **I** was found to be resistant to photolysis on glass and in cyclohexane. A low amount of radiocarbon (1.5%) escaped from the glass surface to the internal surface of the reaction vessel and traps but about half was identified as **I**. The coexistence of the epicuticular waxes did not significantly affect the volatilization loss of radiocarbon but caused photodegradation of **I**. Although the detected amount of degradates were small, **I** underwent oxidative desulfuration, thiono−thiolo rearrangement, and cleavage of the P−O aryl linkage. Dimerization via photoreduction of the nitro group leading to formation of **VI** and **XII** did not occur for **I** in both wax surfaces. In the dark control, 97.2−99.4% of the applied ^{14}C remained as **I** on the Petri dish with a slight volatilization (0.1−4.8%), but insignificant degradation of **I** was observed. When silica gel was used as a carrier, **I** was stable in the dark without volatilization but underwent more photodegradation with formation of **II** (1.0%, 8 h) and unknown degradates (9.9%, 8 h) consisting of many polar fractions of less than 3.8%. The most rapid dissipation of **I** was observed on ODS and PTFE surfaces. The amounts of degradates were minimal, and more amounts of **I** were detected on the internal surface of the reactive vessel or polyurethane foam plug. Similar profiles were observed in the dark but with lower volatilities (<4.2%).

Similar photodegradation studies on glass in the presence or absence of the epicuticular waxes were conducted for **IV**. After 8 h exposure to the artificial light, **IV** that remained in the Petri dish gradually decreased finally to 72−84% of the applied ^{14}C, as listed in **Table 3**. The recovered ^{14}C via volatilization was 2.3−6.4% of the applied ^{14}C, which was slight larger than that of **I**, and most of radiocarbons originated from **IV** unchanged. The main photoproduct on the glass surface was **V** formed via oxidative desulfuration, while the coexistence of the epicuticular waxes caused the formation of **VII** but neither **XI** nor **XIII**. In any case, for **I** and **IV**, mineralization to carbon dioxide was found to be insignificant.

Table 4. CNDO/S Calculations of Fenitrothion (**I**) and Parathion (**IV**)

	I		IV		
wavelength (nm)	280.16		288.10		
oscillator strength	0.1247		0.2674		
main transition (CI coeff)	NHOMO→LUMO (54%)		HOMO→LUMO (50%) NHOMO→LUMO (37%)		
MO	NHOMO	LUMO	NHOMO	HOMO	LUMO
energy level (eV)	−10.558	−2.952	−10.798	−10.503	−3.129
electron density	phenyl-π (90.4%)	NO_2-π* (62.0%)	phenyl-π (82.5%)	phenyl-π (75.6%)	NO_2-π* (74.6%)
Δcharge[a]					
N	−0.3416		−0.3263		
O	−0.1232		−0.1611		
O	−0.1113		−0.1600		

[a] Difference of atomic charge in the nitro group by excitation.

CALCULATION

The PM3 geometry optimization gave similar conformations for **I** and **IV**, where the phenyl ring and one alkyl chain oriented in gauche positions to the P═S moiety ($-SPOC_{(ph)}$, −62.5° (**I**) and −65.0° (**IV**); $-SPOC_{(alkyl)} = -50.3°$ (**I**, **IV**)). The other alkyl group was in the trans position (−178.0° (**I**), −168.8° (**IV**)). The torsional angle of the phenyl ring was determined to be 91.1° (**I**) and 91.4° (**IV**). The results of CNDO/S calculations for **I** and **IV** based on these optimized orientations are summarized in **Table 4**. The absorption maxima were estimated to be slightly larger by approximately 20 nm than those in UV spectra, which was considered to stem from a neglect of solvent effect. These absorptions were considered mainly electronic transitions from the highest occupied MO (HOMO) to the lowest unoccupied MO (LUMO) and or from next HOMO (NHOMO) to LUMO. These occupied MOs were found to locate at the phenyl ring as π-orbitals, and LUMO was dominantly found at the nitro groups (π*-orbital). Therefore, these transitions were considered to have a charge-transfer character. The analysis of the atomic charge difference through these transitions showed the increase of a negative charge in the nitro group. More negative charge on oxygen atoms of the nitro group in **IV** was induced by excitation than in **I**, as shown in **Table 4**.

DISCUSSION

Organophosphorus pesticides are known to undergo photoinduced oxidative desulfuration, thiono−thiolo rearrangement, and cleavage of the P−O aryl linkage on the various types of solid surface including plant (*2*). Photodegradation of **I** did not proceed in aprotic cyclohexane similarly to **IV**, as reported by Schwack et al. (*3*). The glass surface was found to be inactive for **I**, but the photodegradation of **IV** was observed, although similar half-lives (7.4 days) have been reported for **I** and **IV** in photodegradation at 300 nm (*26*).

In the cases of ODS and PTFE, which are considered to have less adsorption ability to a chemical, the main route of dissipation from the Petri dish was volatilization. Alternatively, silica gel having reactive silanol groups in its surface gave a photoreactive environment for **I** but most of the degradates were unknown polar ones. In contrast, **I** underwent the photochemical reactions described above, that was similar to its metabolism in tomato plants (*27*). These results showed that simple aliphatic organic solvent, inert surfaces such as glass, ODS, and PTFE, and reactive silica gel were not appropriate for a model surface of a plant.

Schwack (*14*) has reported the mechanism for photoinduced formation of **VII**. Through investigation using unsaturated organic solvents and enzymatically isolated cuticles, the photoinduced reductions of the nitro group were found to proceed in favor of the usual oxidative desulfuration and cleavage of the P−O aryl linkage (*4*). The reactive intermediates such as nitroso and hydroxylamine derivatives were considered to undergo further reactions with the amino derivative finally to form azo and azoxy derivatives. Our study using the fruit and leaf epicuticular wax of tomato could identify the formation of **VII** from **IV**, but any reduced or dimerized derivatives could not be detected through photodegradation of **I**. Therefore, this difference was most likely to stem from the charge of an intrinsic photoreactivity for **I**. IR analysis of **I** and **IV** in the presence of the epicuticular waxes demonstrated the shift of the NO_2 absorption due to asymmetric stretching slightly to higher wavenumbers. A similar shift has been reported for trifluralin absorbed onto clay matrix (*28*), and this change was considered to originate from the interaction between the nitro oxygen and the silanol group of the clay surface. As reported by Schwack et al. (*3*), the photoreduction of **IV** was considered to proceed in the aid of plant waxes or organic solvents as a proton source. Incidentally, our observation indicated both **I** and **IV** would exist by their nitro groups interacting with components of the epicuticular waxes. CNDO/S calculations showed NHOMO−LUMO or HOMO−LUMO transition predominant via excitations of **I** and **IV**, which caused a partial electron transfer from the phenyl ring to the nitro group. However, this charge transfer was found more for **IV** than **I**, which might make the nitro group of **IV** more facile to be reduced under irradiation.

In the presence of tomato epicuticular waxes, both **I** and **IV** interact with their components at the nitro group which participates in the photoreduction, but the small structural differences between **I** and **IV** were considered to play a great role in their photoreactivity, as demonstrated by molecular orbital calculations.

LITERATURE CITED

(1) Walton, T. J. *Waxes, Cutin and Suberin, Methods in Plant Biochemistry*, Vol.4; Academic Press: New York, 1990; Chapter 5.

(2) Katagi, T. Photodegradation of pesticides on plant and soil surfaces. *Rev. Environ. Contam. Toxicol*. **2004**, *182*, 1−195.

(3) Schwack, W.; Andlauer, W.; Armbruster, W. Photochemistry of parathion in the plant cuticle environment: Model reactions in the presence of 2-propanol and methyl 12-hydroxystearate. *Pestic. Sci*. **1994**, *40*, 279−284.

(4) Schynowski, F.; Schwack, W. Photochemistry of parathion on plant surfaces: Relationship between photodecomposition and iodine number of plant cuticle. *Chemosphere* **1996**, *33*, 2255−2262.

(5) Silva, J.; Ferreira, L.; Silva, A.; Oliveira, A. Photochemistry of 4-chlorophenol on cellulose and silica. *Environ. Sci. Technol*. **2003**, *37*, 4798−4803.
(6) Peacock, G. A.; Riches, M. N.; Wood, S. A new method for the evaluation of the photostability of crop protection compounds; the prediction of photostability in the field. *BCPC Monogr*. **1994**, *59*, 251−256.
(7) Pirisi, F.; Angioni, A.; Cabizza, M.; Cabras, P.; Maccioni, E. Influence of epicuticular waxes on the photolysis of pirimicarb in the solid phase. *J. Agric. Food Chem.* **1998**, *46*, 762−765.
(8) Angioni, A.; Cabizza, M.; Cabras, M.; Melis, M.; Tuberoso, C.; Cabras, P. Effect of the epicuticular waxes of fruits and vegetables on the photodegradation of rotenone. *J. Agric. Food Chem.* **2004**, *52*, 3451−3455.
(9) Cabras, P.; Angioni, A.; Garau, V.; Melis, M.; Pirisi, F.; Minelli, E. Effect of epicuticular waxes of fruits on the photodegradation of fenthion. *J. Agric. Food Chem.* **1997**, *45*, 3681−3683.
(10) Schöenherr, J.; Riederer, M. Plant cuticles sorb lipophilic compounds during enzymatic isolation. *Plant Cell Environ.* **1986**, *9*, 459−466.
(11) Ohkawa, H.; Mikami, N.; Miyamoto, J. Photodecomposition of sumithion [*O*,*O*-dimethyl-*O*-(3-methyl-4-nitrophenyl)-phosphorothioate]. *Agric. Biol. Chem.* **1974**, *38*, 2247−2255.
(12) Greenhalgh, R.; Marshall, W. D. Ultraviolet irradiation of fenitrothion and the synthesis of the photolytic oxidation products. *J. Agric. Food Chem.* **1976**, *24*, 708−713.
(13) Mikami, N.; Imanishi, K.; Yamada, H.; Miyamoto, J. Photodegradation of fenitrothion in water and on soil surface, and its hydrolysis in water. *J. Pestic. Sci.* **1985**, *10*, 263−272.
(14) Schwack, W. Photoreduction of parathion ethyl. *Toxicol. Environ. Chem.* **1987**, *14*, 63−72.
(15) Miyamoto, J.; Kitagawa, K.; Sato, Y. Metabolism of organophosphorus insecticides by *Bacillus subtilis*, with special emphasis on sumithion. *Jpn. J. Exp. Med*. **1966**, *36*, 211−225.
(16) Ahmed, M. K.; Casida, J. E.; Nichols, R. E. Bovine metabolism of organophosphorus insecticides: Significance of rumen fluid with particular reference to parathion. *J. Agric. Food Chem*. **1958**, *6*, 740−746.
(17) Yoshitake, A.; Kawahara, K.; Kodama, T.; Endo, M. Labeled organophosphorus pesticides. I. Synthesis of carbon-14 labeled *O*,*O*-dimethyl *O*-(3-methyl-4-nitrophenyl)phosphorothioate (sumithion). *J. Labelled Compd. Radiopharm.* **1976**, *13*, 323−331.
(18) *Growth stages of mono-and dicotyledonous: Plants BBCH Monograph*, 2nd ed.; Meier, U., Ed.; Federal Biological Research Centre for Agriculture and Forestry: Berlin, Germany, 2001.
(19) McDonald, R.; Nordby, H.; McCollum, T. Epicuticular wax morphology and composition are related to grapefruit chilling injury. *HortScience* **1993**, *28*, 311−312.
(20) Katagi, T. Photoinduced oxidation of the organophosphorus fungicide tolclofos-methyl on clay minerals. *J. Agric. Food Chem.* **1990**, *38*, 1595−1600.
(21) Baker, E. A. Chemistry and morphology of plant epicuticular waxes. *Linn. Soc. Symp. Ser*. **1982**, *10*, 139−165.
(22) Frank, M.; Graebing, P.; Chib, J. Effect of soil moisture and sample depth on pesticide photolysis. *J. Agric. Food Chem.* **2002**, *50*, 2607−2614.
(23) Katagi, T. Ab initio structure of trimethyl- and dimethylphenylphosphorothioates. *J. Mol. Struct.* **1990**, *209*, 61−67.
(24) Stewart, J. J. P. *WINMOPAC Program*; Fujitsu Ltd.: Tokyo, Japan, 2001.
(25) Pople, J. Approximate self-consistent molecular-orbital theory. V. Intermediate neglect of differential overlap. *J. Chem. Phys*. **1967**, *47*, 2026−2033.
(26) Chen, Z.; Zablk, M. Leavltt, comparative study of thin film photodegradative rates for 36 pesticides. *Ind. Eng. Chem. Prod. Res. Dev.* **1984**, *23*, 5−11.
(27) Fukushima, M.; Fujisawa, T.; Katagi, T.; Takimoto, Y. Metabolism of fenitrothion and conjugation of 3-methyl-4-nitrophenol in tomato plant (*Lycopersicon esculentum*). *J. Agric. Food Chem.* **2003**, *51*, 5016−5023.
(28) Margulies, L.; Stern, T.; Rubin, B.; Ruzo, L. Photostabilization of trifluralin adsorbed on a clay matrix. *J. Agric. Food Chem.* **1992**, *40*, 152−155.

Received for review August 26, 2005. Revised manuscript received November 15, 2005. Accepted November 15, 2005.

JF052113D